

# Shaping the Safety Boundaries: Understanding and Defending Against Jailbreaks in Large Language Models

Lang Gao<sup>1,2</sup>, Xiangliang Zhang<sup>3</sup>, Preslav Nakov<sup>1</sup>, Xiuying Chen<sup>1†</sup>

<sup>1</sup>MBZUAI <sup>2</sup>Huazhong University of Science and Technology

<sup>3</sup>University of Notre Dame

{Lang.Gao, Preslav.Nakov, Xiuying.Chen}@mbzuai.ac.ae  
xzhang33@nd.edu

## Abstract

Jailbreaking in Large Language Models (LLMs) is a major security concern as it can deceive LLMs to generate harmful text. Yet, there is still insufficient understanding of how jailbreaking works, which makes it hard to develop effective defense strategies. We aim to shed more light into this issue: we conduct a detailed large-scale analysis of seven different jailbreak methods and find that these disagreements stem from insufficient observation samples. In particular, we introduce *safety boundary*, and we find that jailbreaks shift harmful activations outside that safety boundary, where LLMs are less sensitive to harmful information. We also find that the low and the middle layers are critical in such shifts, while deeper layers have less impact. Leveraging on these insights, we propose a novel defense called **Activation Boundary Defense** (ABD), which adaptively constrains the activations within the safety boundary. We further use Bayesian optimization to selectively apply the defense method to the low and the middle layers. Our experiments on several benchmarks show that ABD achieves an average DSR of over 98% against various forms of jailbreak attacks, with less than 2% impact on the model’s general capabilities.

## 1 Introduction

The widespread use of Large Language Models (LLMs) across various fields (Kaddour et al., 2023) has raised concerns about the safety of the output and the robustness of the model. It has been shown that *jailbreak attacks*, which use crafted prompts to deceive LLMs into generating harmful content, can bypass LLM’s safety alignment (Liu et al., 2024b; Zou et al., 2023), and a lot of research has focused on developing defense mechanisms and counter-prompts to mitigate such attacks (Robey et al., 2023; Xie et al., 2024).

Understanding the internal mechanism of how jailbreaks work is crucial for improving defenses and enhancing safety measures. However, studies explaining jailbreaks remain largely ambiguous and controversial (Yu et al., 2024; Ball et al., 2024a; Lin et al., 2024). From an explainability perspective, debates revolve around which layers are most responsible for a successful attack: He et al. (2024) prioritize the low layers, Zhou et al. (2024); Shen et al. (2024) focus on the middle layers, while Li et al. (2024) highlight the deep layers. Another contradiction lies in whether activations gradually shift as layers deepen or abruptly transition in the middle layers (Zhao et al., 2024a; Shen et al., 2024). Our experiments suggest that these inconsistencies may stem from the limited sample size of prompts, typically around 100, used in prior analyses. From a defense perspective, existing approaches often rely on additional training processes (Zhao et al., 2024a) or probing a limited number of samples (Shen et al., 2024), which affects the utility of LLMs.

Here we aim to better understand the mechanism of how jailbreaking works. In particular, we provide our explanation of jailbreaks based on a comprehensive analysis of over 30,000 samples, a significantly larger scale than previous studies. As an example, Figure 1 shows the two-dimensional projection of three types of prompts: *benign prompts* that contain no harmful information, *harmful prompts* that attempt to induce the LLM to generate harmful content but fail, and various *jailbreak prompts* that successfully induce harmful outputs, collected from different types of jailbreak attack methods. The projection is based on the last token representations across different layers, referred to as *activations*, as they capture the model’s overall understanding of the entire input sequence (Radford et al., 2019; Zou et al., 2023). We can see that different prompts exhibit clustering effects, where the jailbreak activations are distinct from the activation space of harmful prompts. This

<sup>†</sup>Corresponding author.

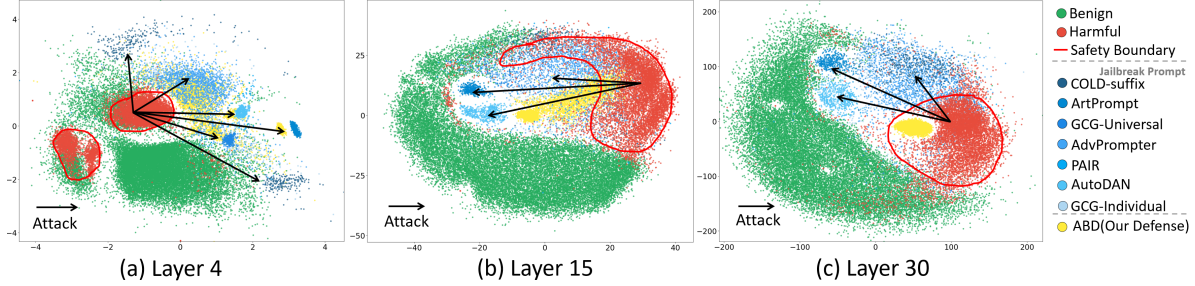


Figure 1: Projected activation space overview of Vicuna-7B-v1.3 across different layers. Harmful activations are observed to cluster together, and we define the surrounding boundary as the *safety boundary*. The attack arrow indicates that jailbreak prompts shift harmful activations into the benign space to evade safety checks.

indicates that in each layer, the LLM performs a rigorous *safety check* within a *safety boundary*, effectively containing most of the harmful activations within this controlled space. Jailbreak prompts, however, bypass these safety checks by shifting activations beyond the safety boundary into an alternative, unmonitored activation space. Notably, the extent of this shift varies across different layers of the LLM, with the low and the middle layers exhibiting the most pronounced effects. This suggests that these layers are critical to the success of jailbreaks.

This finding motivates a new defense mechanism that we propose, **Activation Boundary Defense** (ABD), which constrains jailbreak prompt activations within a safety boundary by applying penalties to activation values. Specifically, we impose minimal penalties within the boundary but sharply increase them beyond it, thereby preserving model utility. The constraint function considers various factors, including the defense layer and the defense dimension, which balance performances on defense and general tasks. We propose a novel adaptive objective that maximizes the Defense Success Rate (DSR) while minimizing the number of penalized layers. This objective is implemented with an adapted Bayesian Optimization (BO) method (Jones et al., 1998; Mockus, 1974), which iteratively proposes and refines selection suggestions.

Experiments on AdvBench (Zou et al., 2023) show that ABD has good generalization, achieving an average DSR of over 98% against various forms of jailbreak attacks. In the general ability tasks, the performance drop of the model equipped with ABD does not exceed 2%, which is significantly lower compared to other defenses, such as 37% for Retokenization (Jain et al., 2023). This demonstrates that our method has a minimal impact

on the model’s overall abilities. In summary, our contributions are threefold:

- We uncover a comprehensive activation distribution and introduce the *safety boundary*, resolving contradictions in prior work and highlighting the vulnerability of the low and the middle layers.
- We propose a lightweight, extensible defense that penalizes only targeted samples and a few key layers, ensuring efficiency and precision.
- Our experiments on benchmark datasets demonstrate that ABD achieves an average DSR of over 98% against various jailbreak attacks, with less than a 2% impact on the general capabilities.

## 2 Related Work

**Jailbreak attacks on LLMs.** Jailbreak attacks craft prompts to induce harmful outputs from LLMs. Early approaches, like DAN (Shen et al., 2023), rely on manually designed prompts. Later research proposed automatic methods. Optimization-based methods (Zou et al., 2023; Liu et al., 2024b; Guo et al., 2024) design optimization strategies to iteratively edit and refine original harmful prompts, enhancing their stealthiness. Model-based methods (Chao et al., 2023; Ding et al., 2024; Paulus et al., 2024) utilize an attacker LLM to autonomously query and refine jailbreak prompts. For rule-based jailbreak methods, Jiang et al. (2024) and Liu et al. (2024c) rewrite prompts using fixed rules that are sufficiently aggressive to deceive the model. In this work, we aim to analyze the mechanisms of these jailbreak methods to develop more effective defense strategies.

**Defense against jailbreak attacks.** Unlike jailbreak methods, defense strategies enhance model safety and robustness by reformulating inputs to counter jailbreak prompts, such as backtranslation (Wang et al., 2024), paraphrasing (Jain et al.,

2023), and reminding (Xie et al., 2023). Some researchers use indicators to distinguish jailbreak prompts, e.g., classify input sequences based on perplexity and sequence length (Alon and Kamfonas, 2023), or classify jailbreak activations using linear classifiers to control whether to answer the query (Zhao et al., 2024a). A new trend in defense involves directly manipulating the representations of the model (Shen et al., 2024; Xu et al., 2024; Li et al., 2024; Liu et al., 2024a) and editing the model (Zhao et al., 2024b), which is more efficient and cost-effective. Unlike these methods, ours avoids extra tokens or modules by directly constraining activations within a safety boundary, ensuring greater efficiency and simplicity.

**Mechanistic interpretability of LLMs.** The growing concern about LLM safety has sparked increasing interest in interpreting LLM features in jailbreak prompts. For example, Ball et al. (2024b) identified a common mechanism whereby jailbreaks reduce the harmfulness perception in most LLMs. Similarly, Li et al. (2024) investigated patterns that trigger the model to recognize safety issues. Zhou et al. (2024) discovered that the vocabulary mappings of activations significantly changed when processing jailbreak inputs. Research efforts have also focused on proposing corresponding defense methods based on interpretability results. For instance, Zhao et al. (2024a) and Shen et al. (2024) model how jailbreak activations transfer between benign and harmful activation spaces as layers deepen. They designed adaptive defenses whose strength varies across different layers. However, the limited data in previous studies often led to controversy and ambiguity. In contrast, we leverage over 30,000 samples to better understand jailbreaks and design effective defenses.

### 3 Understanding Jailbreaks in LLMs

#### 3.1 Controversy in Literature

**What are the key layers?** There have been different opinions about which layers are most important, mainly due to varying perspectives. For example, He et al. (2024) argued that low layers are essential because they treat jailbreak activations as benign ones. Zhou et al. (2024) believe that low and middle layers are essential based on tokens generated from activations. Li et al. (2024) argued that deep layers are critical, as the concept they proposed, called *safety pattern*, has greater values

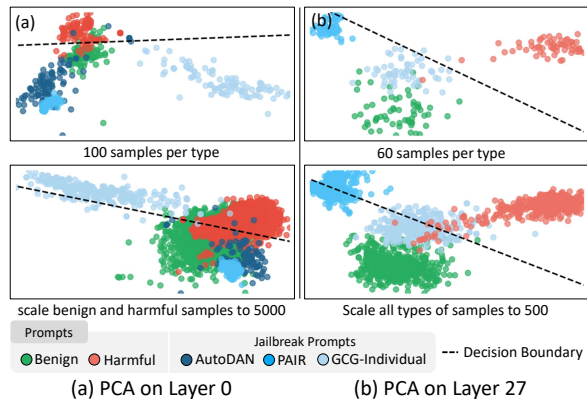


Figure 2: PCA visualization of the activations highlights how conclusions are drawn from tiny sample sizes, such as the side on which the jailbreak activation lies, may not hold with larger datasets. (a) Top: 100 samples per type (following He et al. (2024)); Bottom: Benign and harmful samples increased to 5000. (b) Top: 60 samples per type (similar to Zhao et al. (2024a)); Bottom: All samples increased to 500.

in these layers. Among these works, the first work similarly focuses on activations, as does our paper.

Upon examining their experimental setup, we identified a major limitation: the small number of samples used in the analysis. As shown in Figure 2(a), before scaling the data, benign and harmful activations are linearly separable, with most jailbreak samples being misclassified as benign, which is consistent with the findings from He et al. (2024). However, after scaling the data, half of the jailbreak activations shift to align with harmful ones, and the separation becomes nonlinear. This highlights the risk of misleading from small-scale studies and underscores the importance of large-scale analysis.

**Disputes on the jailbreak mechanism.** There are also different perspectives on the internal mechanism of jailbreak. Specifically, Zhao et al. (2024a) viewed jailbreak as a gradual process where activations transition from harmful to benign spaces from low to deep layers, while Shen et al. (2024) argued that jailbreak abruptly manifests in deeper layers, with activations positioned between harmful and benign spaces. This work used no more than 100 samples per activation type, and we identify a similar issue to the one discussed earlier. Figure 2(b) shows that before scaling the data, the jailbreak activations are aligned to benign activations, which is consistent with findings from Zhao et al. (2024a); while after scaling the data, jailbreaking activations no longer align with either harmful or benign activations. When compared to Shen et al. (2024),



similar conflicting perspectives are observed when scaling up the data. Further details can be found in Appendix C.1. These conflicting perspectives form the basis of the jailbreak mechanisms in these works; their conclusions — such as whether activations gradually shift or abruptly transition — are also questionable.

### 3.2 Experimental Settings

To address the above limitations, we conducted a large-scale analysis on a 300 times greater dataset.

**Dataset.** Our dataset consists of 32,507 samples in three categories: benign, harmful, and jailbreak. For benign samples, we used a subset from the Alpaca dataset (Taori et al., 2023), as it has been carefully curated to ensure that only safe content is included. For harmful samples, we collected five datasets containing harmful queries from RedEval (Bhardwaj and Poria, 2023) and AdvBench (Zou et al., 2023). These datasets encompass a wide variety of harmful prompts designed to elicit unsafe outputs. For jailbreak samples, we applied seven different jailbreak attack methods, including GCG-Individual and GCG-Universal (Zou et al., 2023), AdvPrompter (Paulus et al., 2024), COLD-Suffix Attack (Guo et al., 2024), AutoDAN (Liu et al., 2024b), PAIR (Chao et al., 2023), and ArtPrompt (Jiang et al., 2024), on AdvBench. Detailed statistics can be found in Appendix A.

**Model.** We used Vicuna-7B-v1.3 (Chiang et al., 2023), a 32-layer Transformer model, as the LLM to study. It is tuned upon a safety-aligned LLM and is able to identify certain harmful prompts. However, as demonstrated in previous work (Chu et al., 2024), it can also be easily deceived and generate harmful information during jailbreak attacks. This makes it an excellent example for studying both attack mechanisms and defense strategies.

**MDS projection.** Our projection was based on the *activation*, the last token vector of the input, as it captures the model’s overall understanding of the entire input sequence (Radford et al., 2019; Zou et al., 2023). As discussed in §3.1, linear classification may be insufficient to model the boundary between different prompts. Therefore, we adopted Multi-Dimensional Scaling (MDS) (Carroll and Arabie, 1998) as our dimensionality reduction method, as MDS is more effective than PCA in handling large-scale and complexly distributed data (Anowar et al., 2021). Moreover, it better cap-

tures the global distribution structure compared to t-SNE (Van der Maaten and Hinton, 2008).

### 3.3 Jailbreak Mechanisms Findings

#### 3.3.1 Activation Distribution

We present the activation distributions of representative layers in Figure 1, with the full version available in Appendix B. Our key observations are as follows: (1) *Harmful and benign activations overlap and are not linearly separable in most layers, especially in low and middle layers*, as shown in Figure 1(a) and Figure 1(b), where benign and harmful activations are overlapping with no clear linear decision boundaries to separate them. This highlights the intricate interplay between harmful and benign activations, indicating that forcing jailbreak activations into a linear benign-vs-harmful classification is impractical. (2) *Jailbreak activations significantly shift out of the harmful activation space in most layers*, forming an independent region with low overlap with harmful activations. This pattern is consistent across various jailbreaks, suggesting that jailbreaks achieve deception by shifting activations. Such shift is evident in all layers, indicating that jailbreaks begin in low layers and continue to affect the model across all layers, rather than starting in middle or deep layers (Zhou et al., 2024; Shen et al., 2024). Moreover, the shift is the most pronounced in the low and middle layers, implying their importance in jailbreaks.

#### 3.3.2 Safety Boundary

Based on the observation of jailbreak and harmful activations, we propose the following hypothesis: A safety boundary exists that ensures sensitivity to harmful content within its activation space, but jailbreak prompts can bypass it, generating harmful responses. To verify the existence of the safety boundary, we conduct experiments and present two concepts described below.

We first explore Randomized Activation Shifting (RAS), an approximation of jailbreak attacks that introduces a random value shift to the original activation. Specifically, assuming the activation on the  $l$ -th layer is  $a_l$ , we shift it by a distance  $r$  in a random direction  $\hat{u}$ :

$$a_l \leftarrow a_l + r \cdot \hat{u}. \quad (1)$$

Figure 3(a) shows the changes in Defense Success Rate (DSR) under different values of  $r$  for four selected layers. The definition of this metric is

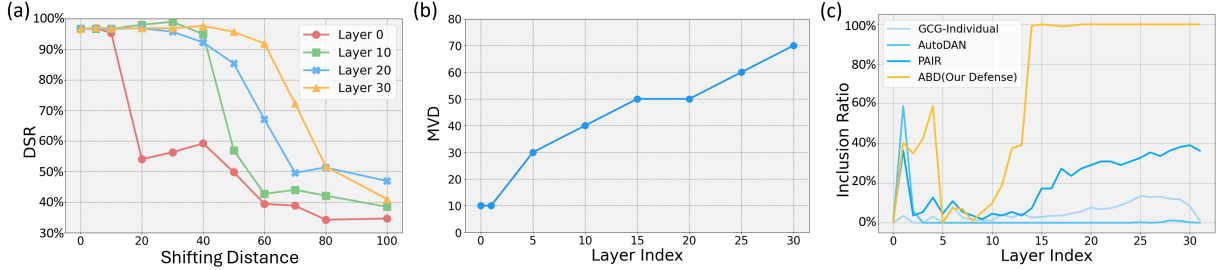


Figure 3: (a) Impact of random activation shifts across layers. DSR (Defense Success Rate) decreases as shifting distance increases, regardless of the affected layers. (b) MVD (Most Vulnerable Distance) across layers. MVD increases as layers go deeper. (c) Inclusion ratio of jailbreaking activations in the harmful activation space. Without ABD, the ratio stays below 0.4 but rises to 1 when ABD is applied.

provided in the Appendix. Initially, when  $r = 0$ , the corresponding DSR is over 99%, as the harmful text has activations within the safety boundary. Then, as the distance  $r$  increases, the DSR decreases for all layers, indicating that harmful activations become harder for the model to detect. Notably, regardless of the selected layer, a steep drop in DSR is observed at a specific range (e.g.,  $r = 10 - 20$  on layer 0), while the decline is more moderate in other regions. This observation suggests *the presence of a safety boundary*.

For more accurate boundary detection, we provide the second visualization, which introduces a measurable concept called Most Vulnerable Distance (MVD) as an approximation of the boundary. MVD represents the specific distance at which the DSR experiences the steepest drop, indicating the point where the model’s ability to detect harmful activations becomes most vulnerable:

$$\text{MVD} = \arg \min_r \frac{d(\text{DSR})}{dr}, \quad (2)$$

where  $\frac{d(\text{DSR})}{dr}$  denotes the rate of change of DSR with respect to  $r$ . As shown in Figure 3(b), MVD increases with the depth of the model’s layers. This implies that *the safety boundary also expands in deeper layers*, requiring more substantial shifts to compromise the model’s safety checks. The findings align closely with our intuitive observations in Figure 1. Figure 1(a) shows that in low layers, jailbreak activations are shifted in various directions, but all evidently surpass the safety boundary. In the middle layers presented in Figure 1(b), most jailbreak activations are beyond the safety boundary, and they are more aligned with benign activations. In the deep layers shown in Figure 1(c), jailbreak activations cluster within a region, which overlaps a little with the safety boundary.

### 3.3.3 Key Takeaways on the Jailbreak Process

Based on the above analysis, we summarize the jailbreak process as follows: (1) Jailbreak takes effect in the low layers, contrary to prior work (Zhou et al., 2024), which suggested it begins in the middle layers. (2) As the attack progresses, jailbreak continues to operate, shifting the activation outside the safety boundary and causing the model to be deceived. (3) When comparing all layers, the low and the middle layers exhibit the strongest shift and smallest safety boundaries, demonstrating their importance in the jailbreak process.

## 4 Activation Boundary Defense

Based on the above findings, we propose a defense called Activation Boundary Defense (ABD), whose core idea is to confine the activations within the safety boundaries. The workflow of ABD is shown in Figure 4. ABD includes a penalty function and a Bayesian optimization process. The penalty constrains activations within safety boundaries, while Bayesian optimization iteratively adjusts the affected layers and the penalty parameters.

### 4.1 Penalty Function

**Overall design of penalty.** Intuitively, an activation stays within the safety boundary if all its coordinates lie within a regular range; in contrast, outliers have at least one coordinate exceeding this range. Adjusting these outlier coordinates can guide the activations back within the boundary. Since directly measuring the safety boundaries is challenging and rigid constraints risk disrupting model operations, we apply a smooth penalty, adjusting the outlier coordinates while leaving the normal ones unaffected.

#### Approximation of activation distributions.

We empirically find that the activation distributions

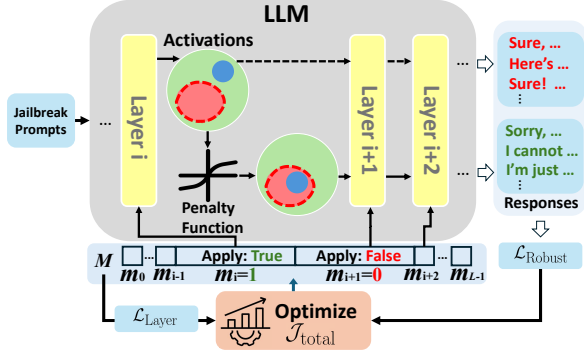


Figure 4: Workflow of ABD. ABD restricts outlier activation coordinates using a penalty function and determines its application scope via BO-based tuning.

in each layer can be approximated by a normal distribution. The proof is as follows. For each layer  $l$ , we examine two distributions: the activation coordinate distribution  $\mathcal{D}^l(x)$  and a normal distribution  $\mathcal{D}_{\mathcal{N}}^l(x)$  with the same mean  $\mu_{\mathcal{D}}^l$  and standard deviation  $\sigma_{\mathcal{D}}^l$ . To measure their similarity, we compute the Jensen-Shannon (JS) divergence (Lin, 1991) between  $\mathcal{D}^l(x)$  and  $\mathcal{D}_{\mathcal{N}}^l(x)$ . Across all layers, the maximum JS divergence is 0.0839, and the mean is 0.0575, and both are well below 0.1. These low JS divergence values indicate strong similarity between  $\mathcal{D}^l(x)$  and  $\mathcal{D}_{\mathcal{N}}^l(x)$ , which supports the validity of approximating  $\mathcal{D}^l(x)$  with  $\mathcal{D}_{\mathcal{N}}^l(x)$ .

**Penalty function design.** To design a practical penalty function for activation coordinates, we establish three key principles: (1) It should target only outlier activations, leaving non-outliers unaffected. (2) The penalty should grow with the magnitude of deviation, reflecting distance-based penalization. (3) The function must be computationally efficient.

To construct penalty functions compatible with the activation coordinate distribution  $\mathcal{D}^l(x)$ , we approximate it using  $\mathcal{D}_{\mathcal{N}}^l(x)$  and focus on two geometric properties. First, *symmetry around the mean value*  $\mu_{\mathcal{D}}^l$  requires the penalty function also to be symmetric about  $\mu_{\mathcal{D}}^l$ , ensuring unbiased penalization of outliers above or below the safety boundary. Second, *the nonlinear decay of probability density* with increasing distance from  $\mu_{\mathcal{D}}^l$  implies that the penalty should grow nonlinearly with the distance, rising faster than a linear penalty. Following these principles, we propose a penalty function that updates the original activation coordinate scalar value  $x$  to  $x'$  as follows:

$$x' = \alpha^l \cdot \tanh(\beta^l \cdot (x - \mu_{\mathcal{D}}^l)) + \mu_{\mathcal{D}}^l, \quad (3)$$

where  $\alpha^l \geq 0$  and  $\beta^l \geq 0$  are hyperparameters. Visualization is given in Appendix D.1.

This function meets the stated expectations. It is symmetric about the mean  $\mu_{\mathcal{D}}^l$ , ensuring fair penalization for deviations above and below this central value. The penalty strength  $|x - x'|$  increases nonlinearly with the distance from  $\mu_{\mathcal{D}}^l$  because  $\tanh(\cdot)$  amplifies more significant deviations with its steep slope, reflecting stronger penalization for outliers. Moreover, the function mostly penalizes outliers. Within the range  $[\mu_{\mathcal{D}}^l - b^l, \mu_{\mathcal{D}}^l + b^l]$ ,  $x' \approx x$ , resulting in a negligible penalty for values close to the mean. The hyperparameters  $\alpha^l$  and  $\beta^l$  govern the behavior of the penalty function. The parameter  $\alpha^l$  determines the maximum range of  $x'$ , ensuring all coordinates are constrained within  $(-\alpha^l + \mu_{\mathcal{D}}^l, \alpha^l + \mu_{\mathcal{D}}^l)$  after penalty application. Meanwhile,  $\beta^l$  controls the size of the unmodified region  $[\mu_{\mathcal{D}}^l - b^l, \mu_{\mathcal{D}}^l + b^l]$ ; increasing  $\beta^l$  expands this region, while decreasing  $\beta^l$  narrows it.

## 4.2 Bayesian Optimization-Based Tuning

Another crucial aspect of our method is the configuration of the hyperparameters and the application scope of the penalty function. Specifically, we must (1) minimize the number of affected activation coordinates to limit unnecessary perturbations, and 2) for each affected layer  $l$ , find the values of  $\alpha^l$  and  $\beta^l$  that best improve the model’s resilience against adversarial attacks. To accomplish these goals, we use a Bayesian Optimization (BO)-based (Jones et al., 1998; Mockus, 1974) tuning method. Concretely, we define two core objectives.

**Layer selection objective:** We introduce a tunable mask  $M = [m_0, \dots, m_{L-1}]$ ,  $m_i \in \{0, 1\}$ , where  $m_i = 1$  indicates that ABD is applied to layer  $i$ . Here,  $L$  is the total number of transformer layers. By minimizing the ratio of layers where ABD is active, we reduce the number of interventions:

$$\mathcal{L}_{\text{Layer}} = 1 - \frac{\text{Sum}(M)}{L}. \quad (4)$$

**Robustness objective:** For each layer  $l$  with ABD applied, we aim to find  $\alpha^l$  and  $\beta^l$  to maximize the defense. A hyperparameter  $k^l \in (0, 1]$  controls the fraction of penalized activation coordinates, with smaller  $k^l$  reducing disturbance but potentially weakening ABD. These parameters are aggregated as  $\Theta = \{\theta^l \mid l \in [0, L - 1]\}$ , where  $\theta^l = \alpha^l, \beta^l, k^l$ . The robustness objective is as follows:

$$\mathcal{L}_{\text{Robust}} = \text{DSR}(\text{Model}(\cdot \mid \Theta, M)). \quad (5)$$

Model	Jailbreak	No Defense	Paraphrase	PPL	Retokenization	SafeDecoding	Self-Exam	Self-Reminder	ABD (Ours)
Vicuna	No attack	88%	82%	90%	66%	88%	100%	100%	100%
	GCG-Individual	4%	86%	78%	62%	100%	86%	100%	100%
	AutoDAN	6%	26%	12%	36%	78%	30%	30%	44%
	PAIR	30%	62%	40%	30%	94%	86%	100%	76%
	DeepInception	10%	2%	2%	0%	98%	18%	40%	58%
Llama-2	No attack	100%	100%	100%	94%	100%	100%	100%	100%
	GCG-Individual	50%	98%	100%	98%	100%	64%	100%	100%
	AutoDAN	98%	94%	98%	94%	100%	100%	98%	100%
	PAIR	72%	90%	82%	78%	92%	100%	86%	92%
	DeepInception	74%	82%	88%	60%	100%	94%	96%	100%

Table 1: The Defense Success Rate (DSR) of different defense methods across Vicuna-7B-v1.3 (simplified as Vicuna) and Llama-2-7B-chat (simplified as Llama-2) along with different attack types, where a higher DSR indicates better defense effectiveness. For ABD, the **best** and **second** performance across all defenses are highlighted.

Since decreasing  $k^l$  too aggressively can weaken ABD’s defense, our main strategy for reducing perturbations to the model is to minimize the number of affected layers by controlling the mask  $M$ . Our final objective is a weighted sum of two objectives:

$$\mathcal{J}_{\text{total}}(\Theta, M) = w \cdot \mathcal{L}_{\text{Robust}} + (1 - w) \cdot \mathcal{L}_{\text{Layer}},$$

where  $w$  is a manually set parameter balancing defense robustness and minimal intervention.

## 5 Experiments

### 5.1 Settings

**Backbone models.** We consider two widely used open-source LLMs as the target models in our experiments: Llama-2-7B-Chat (Touvron et al., 2023) and Vicuna-7B-v1.3. Llama-2-7B-Chat is specially trained for safety alignment, while Vicuna-7B-v1.3 is tuned based on Llama without extra alignment for safety. The configurations of the LLMs are shown in Appendix E.1.

**Jailbreak and defense baselines.** For *jailbreak methods*, we considered four widely applied ones: optimization-based methods include GCG-Individual and AutoDAN, which iteratively optimize a jailbreak prompt towards the goal of generating affirmative responses. Model-based jailbreak, i.e., PAIR, uses an attacker LLM to refine the jailbreak prompts. The rule-based method includes DeepInception (Li et al., 2023), which crafts jailbreak prompts based on a stealthy template. Correspondingly, we applied different *defense methods* to the models to compare them to our model for combating jailbreak methods: Paraphrase (Jain et al., 2023), Retokenization (Jain et al., 2023) and Self-Reminder (Xie et al., 2023) reformulate the input to avoid attack; PPL (Alon and Kamfonas, 2023) and Self-Exam (Phute et al., 2023) defense

LLMs by double-checking their outputs; SafeDecoding (Xu et al., 2024) uses a tuned model to modify the output probability distribution.

**Datasets and metrics.** Following Xu et al. (2024) and Chao et al. (2023), we utilized 50 samples from AdvBench (Zou et al., 2023) as the test set. We used DSR when evaluating defense effectiveness. Furthermore, following Xu et al. (2024), we adopted Just-Eval (Lin et al., 2023) to measure the general abilities of LLMs before and after applying defense. Just-Eval is a comprehensive benchmark containing 1,000 diverse instructions, covering seven task types (e.g., reasoning, math, coding, etc.) and seven topics (e.g., ethics, nature, STEM, etc.). Following Lin et al. (2023), we leveraged GPT-4o-mini (OpenAI, 2024) to score the quality of the outputs, ranging from 1 to 5, across five aspects: helpfulness, clarity, factuality, depth, and engagement. We reported the average score for each aspect and the overall average score for different aspects, denoted as Avg. To evaluate the efficiency, we calculated the Runtime per Query for each defense, which represents the average time taken to process a single query during inference. This metric provides a direct measurement of the efficiency of defenses in real-world applications. We also utilized the above two metrics to derive an overall score that simultaneously reflects LLMs’ responding speed and quality. The calculation is shown in Appendix E.4.1.

**Implementation Details.** We randomly filtered 400 non-overlapping AdvBench samples to compute  $\mu_D^l$  and used them as a validation set. We used GCG-Universal (Zou et al., 2023) to attack the validation set. GCG-Universal finds a shared jailbreak suffix for all harmful prompts that can deceive LLMs. By default, we set  $w = 0.7$  when



Defense	Runtime per Query↓	Just-Eval↑						Overall↑
		Helpfulness↑	Clarity↑	Factuality↑	Depth↑	Engagement↑	Avg.↑	
No Defense	2.291	3.478	3.784	3.870	2.521	2.743	3.279	0.767
Paraphrase	2.897	3.397	3.769	3.911	2.549	2.737	3.273	0.477
PPL	1.843	2.156	2.719	2.958	1.501	1.911	2.249	0.576
Retokenization	1.964	1.933	2.463	2.659	1.379	1.845	2.056	0.442
SafeDecoding	2.239	3.231	3.732	3.885	2.367	3.009	3.245	0.778
Self-Exam	2.449	3.449	3.812	3.940	2.542	2.705	3.290	0.696
Self-Reminder	2.205	2.109	2.641	2.988	1.481	1.980	2.240	0.400
ABD (Ours)	2.302	3.533	3.774	3.973	2.573	2.806	3.332	0.782

Table 2: Comparison of defenses on Runtime per Query and Just-Eval metrics in Vicuna-7B-v1.3. ↓: smaller is better; ↑: larger is better. For ABD, the **best** and **second** performances are highlighted. ABD preserves the model’s general performance, adding less than 0.1 seconds to runtime while producing high-quality outputs with leading evaluation scores. It has the best overall performance across all defenses.

calculating  $\mathcal{L}_{\text{Robust}}(\Theta, M)$  to slightly prioritize improving DSR while balancing defensive capability and perturbation to LLMs. Appendix D.2 presents more details about ABD optimization.

## 5.2 Experimental Results

**ABD reveals vulnerabilities in low and middle layers.** In both models, low and middle layers, such as layers 5 and 12 in Vicuna-7B-v1.3 and layers 2 and 12 in Llama-2-7B-chat, are penalized, which aligns with our observed findings and proposed explanation that low and middle layers are more vulnerable to jailbreak attacks due to noticeable activation shifts.

**ABD successfully constrains jailbreak activations.** Figure 3(c) shows the percentage of jailbreak activations within the harmful activation space, namely the inclusion ratio. Before applying ABD, the inclusion ratio remains below 0.4 for various jailbreak activations, indicating that jailbreak activations lie outside of the safety boundary. After applying ABD, the ratio increases to 1, demonstrating that our method effectively constrains the jailbreak activations within the safety boundary. Additional details are provided in Appendix C.2. From a visualization perspective, Figure 1 projects activations for different prompts. Under our defense, jailbreak activations are progressively constrained within the harmful activation space under ABD, as shown in Figure 1. further confirming the effectiveness of ABD for mitigating jailbreak effects.

**Statistic effectiveness of ABD.** We report the statistical defense results of ABD on the test set in Table 1. For Vicuna-7B-v1.3, which lacks specific safety alignment, the defense poses a more challenging task. Nevertheless, ABD demonstrates

competitive performance. For jailbreak methods such as PAIR and DeepInception, ABD achieves a higher DSR (58%) compared to Paraphrase (2%) and Retokenization (0%), both of which require costly prompt reformulation. Against the GCG-Individual attack, ABD successfully defends against all jailbreak samples. For the well-aligned model Llama-2-7B-chat, ABD achieves 100% DSR under most jailbreak methods.

**ABD is efficient and reliable.** Table 2 shows Runtime per Query, Just-Eval scores, and overall scores of Vicuna-7B-v1.3 with different defenses applied. We find that ABD has the greatest overall score across all defenses. Moreover, ABD only adds marginal extra time cost and general ability affection. Specifically, it only causes less than 1% delay in each sample and less than 2% perturbation in overall ability, compared to costly methods such as Paraphrase and Self-Exam. Furthermore, with ABD applied, the helpfulness, actuality, depth, and engagement also show a slight increase. We further discover that for baseline defenses such as Retokenization and Self-Reminder, LLM would generate overly simplistic outputs, which leads to smaller Runtime per Query, but they have significantly smaller Just-Eval scores.

## 6 Conclusion and Future Work

We conducted a comprehensive study of jailbreak mechanisms, analyzing over 30,000 samples. Our findings reveal that jailbreak shifts harmful activations outside the safety boundary in each layer, with the most severe shifts occurring in the low and middle layers. Motivated by this finding, we proposed ABD, which drives jailbreak activations back within the safety boundary, utilizing LLMs’ intrinsic sensitivity to harmful information. Our



experiments suggest that ABD is both practical and efficient. In the near future, we aim to investigate the safety challenges of jailbreak attacks in multi-turn dialogue systems.

## Limitations

### Underperformance in under-aligned models.

For certain attack methods, under-aligned models (Vicuna-7B-v1.3) may not perform significantly as well-aligned models (Llama2-7B-chat). We believe this is because under-aligned models have unclear safety boundaries, which complicate the search for penalty functions that balance general ability and DSR. Future work could refine ABD by specifically searching for activation spaces that preserve the concept of "safety", therefore enhancing its generalizability on uncensored models.

**Focus on single-round jailbreak.** In this study, we primarily focus on single-round jailbreak scenarios. We do not extend our analysis to more complex jailbreaks that involve long contexts or multi-round dialogues, such as CFA (Sun et al., 2024). As a result, the relationship between jailbreak dialogues and safety boundaries remains largely unexplored. Addressing this limitation, we plan to investigate and incorporate methods for detecting safety boundaries in multi-round dialogue scenarios as part of our future work.

## Ethical Considerations

The aim of this research is to enhance the explainability and safety of LLMs. Our proposed jailbreak mechanism, that jailbreak shift activations out of the safety boundary, can mitigate disputes on how jailbreak happens and promote the development of both LLM explainability and safety. We highlight that the development of ABD only needs publicly available datasets and jailbreak methods and does not require designing new jailbreak methods. We demonstrate some harmful responses from LLMs only for illustration purposes. We acknowledge that ABD would cause the development of new attacks. Therefore, we will explore using random perturbation in the input sequence rather than a particular jailbreak method when optimizing to mitigate such attacks.

## References

Takuya Akiba, Shotaro Sano, Toshihiko Yanase, Takeru Ohta, and Masanori Koyama. 2019. Optuna: A next-

generation hyperparameter optimization framework. In *The 25th ACM SIGKDD International Conference on Knowledge Discovery & Data Mining*, pages 2623–2631.

Gabriel Alon and Michael Kamfonas. 2023. Detecting language model attacks with perplexity. *arXiv preprint arXiv:2308.14132*.

Farzana Anowar, Samira Sadaoui, and Bassant Selim. 2021. Conceptual and empirical comparison of dimensionality reduction algorithms (pca, kpca, lda, mds, svd, lle, isomap, le, ica, t-sne). *Computer Science Review*, 40:100378.

Sarah Ball, Frauke Kreuter, and Nina Panickssery. 2024a. Understanding jailbreak success: A study of latent space dynamics in large language models. *arXiv preprint arXiv:2406.09289*.

Sarah Ball, Frauke Kreuter, and Nina Panickssery. 2024b. Understanding jailbreak success: A study of latent space dynamics in large language models. *Preprint*, arXiv:2406.09289.

Rishabh Bhardwaj and Soujanya Poria. 2023. Red-teaming large language models using chain of utterances for safety-alignment. *Preprint*, arXiv:2308.09662.

J Douglas Carroll and Phipps Arabie. 1998. Multi-dimensional scaling. *Measurement, judgment and decision making*, pages 179–250.

Patrick Chao, Alexander Robey, Edgar Dobriban, Hamed Hassani, George J. Pappas, and Eric Wong. 2023. Jailbreaking black box large language models in twenty queries. *Preprint*, arXiv:2310.08419.

Wei-Lin Chiang, Zhuohan Li, Zi Lin, Ying Sheng, Zhanghao Wu, Hao Zhang, Lianmin Zheng, Siyuan Zhuang, Yonghao Zhuang, Joseph E. Gonzalez, Ion Stoica, and Eric P. Xing. 2023. Vicuna: An open-source chatbot impressing gpt-4 with 90%\* chatgpt quality.

Junjie Chu, Yugeng Liu, Ziqing Yang, Xinyue Shen, Michael Backes, and Yang Zhang. 2024. Comprehensive assessment of jailbreak attacks against llms. *arXiv preprint arXiv:2402.05668*.

Peng Ding, Jun Kuang, Dan Ma, Xuezhi Cao, Yunsen Xian, Jiajun Chen, and Shujian Huang. 2024. A wolf in sheep’s clothing: Generalized nested jailbreak prompts can fool large language models easily. In *Proceedings of the 2024 Conference of the North American Chapter of the Association for Computational Linguistics: Human Language Technologies (Volume 1: Long Papers)*, pages 2136–2153, Mexico City, Mexico. Association for Computational Linguistics.

Xingang Guo, Fangxu Yu, Huan Zhang, Lianhui Qin, and Bin Hu. 2024. Cold-attack: Jailbreaking llms with stealthiness and controllability. *arXiv preprint arXiv:2402.08679*.

- Zeqing He, Zhibo Wang, Zhixuan Chu, Huiyu Xu, Rui Zheng, Kui Ren, and Chun Chen. 2024. [Jailbreaklens: Interpreting jailbreak mechanism in the lens of representation and circuit](#). *Preprint*, arXiv:2411.11114.
- Neel Jain, Avi Schwarzschild, Yuxin Wen, Gowthami Somepalli, John Kirchenbauer, Ping-yeh Chiang, Micah Goldblum, Aniruddha Saha, Jonas Geiping, and Tom Goldstein. 2023. Baseline defenses for adversarial attacks against aligned language models. *arXiv preprint arXiv:2309.00614*.
- Fengqing Jiang, Zhangchen Xu, Luyao Niu, Zhen Xiang, Bhaskar Ramasubramanian, Bo Li, and Radha Poovendran. 2024. [ArtPrompt: ASCII art-based jailbreak attacks against aligned LLMs](#). In *Proceedings of the 62nd Annual Meeting of the Association for Computational Linguistics (Volume 1: Long Papers)*, pages 15157–15173, Bangkok, Thailand. Association for Computational Linguistics.
- Donald R Jones, Matthias Schonlau, and William J Welch. 1998. Efficient global optimization of expensive black-box functions. *Journal of Global optimization*, 13:455–492.
- Jean Kaddour, Joshua Harris, Maximilian Mozes, Herbie Bradley, Roberta Raileanu, and Robert McHardy. 2023. Challenges and applications of large language models. *arXiv preprint arXiv:2307.10169*.
- Tianlong Li, Xiaoqing Zheng, and Xuanjing Huang. 2024. Rethinking jailbreaking through the lens of representation engineering. *ArXiv preprint, abs/2401.06824*.
- Xuan Li, Zhanke Zhou, Jianing Zhu, Jiangchao Yao, Tongliang Liu, and Bo Han. 2023. Deepinception: Hypnotize large language model to be jailbreaker. *arXiv preprint arXiv:2311.03191*.
- Bill Yuchen Lin, Abhilasha Ravichander, Ximing Lu, Nouha Dziri, Melanie Sclar, Khyathi Chandu, Chandra Bhagavatula, and Yejin Choi. 2023. [The unlocking spell on base llms: Rethinking alignment via in-context learning](#). *ArXiv preprint*.
- Jianhua Lin. 1991. Divergence measures based on the shannon entropy. *IEEE Transactions on Information theory*, 37(1):145–151.
- Yuping Lin, Pengfei He, Han Xu, Yue Xing, Makoto Yamada, Hui Liu, and Jiliang Tang. 2024. [Towards understanding jailbreak attacks in LLMs: A representation space analysis](#). In *Proceedings of the 2024 Conference on Empirical Methods in Natural Language Processing*, pages 7067–7085, Miami, Florida, USA. Association for Computational Linguistics.
- Quan Liu, Zhenhong Zhou, Longzhu He, Yi Liu, Wei Zhang, and Sen Su. 2024a. [Alignment-enhanced decoding: Defending jailbreaks via token-level adaptive refining of probability distributions](#). In *Proceedings of the 2024 Conference on Empirical Methods in Natural Language Processing*, pages 2802–2816, Miami, Florida, USA. Association for Computational Linguistics.
- Xiaogeng Liu, Nan Xu, Muhao Chen, and Chaowei Xiao. 2024b. [Autodan: Generating stealthy jailbreak prompts on aligned large language models](#). In *The Twelfth International Conference on Learning Representations*.
- Yue Liu, Xiaoxin He, Miao Xiong, Jinlan Fu, Shumin Deng, and Bryan Hooi. 2024c. [Flipattack: Jailbreak llms via flipping](#). *Preprint*, arXiv:2410.02832.
- Jonas Mockus. 1974. On bayesian methods for seeking the extremum. In *Proceedings of the IFIP Technical Conference*, pages 400–404.
- OpenAI. 2024. [Gpt-4o mini: Advancing cost-efficient intelligence](#).
- Anselm Paulus, Arman Zharmagambetov, Chuan Guo, Brandon Amos, and Yuandong Tian. 2024. Advprompter: Fast adaptive adversarial prompting for llms. *arXiv preprint arXiv:2404.16873*.
- Mansi Phute, Alec Helbling, Matthew Hull, ShengYun Peng, Sebastian Szyller, Cory Cornelius, and Duen Horng Chau. 2023. Llm self defense: By self examination, llms know they are being tricked. *arXiv preprint arXiv:2308.07308*.
- Alec Radford, Jeffrey Wu, Rewon Child, David Luan, Dario Amodei, Ilya Sutskever, et al. 2019. Language models are unsupervised multitask learners. *OpenAI blog*, 1(8):9.
- Alexander Robey, Eric Wong, Hamed Hassani, and George J Pappas. 2023. Smoothllm: Defending large language models against jailbreaking attacks. *arXiv preprint arXiv:2310.03684*.
- Guobin Shen, Dongcheng Zhao, Yiting Dong, Xiang He, and Yi Zeng. 2024. Jailbreak antidote: Runtime safety-utility balance via sparse representation adjustment in large language models. *arXiv preprint arXiv:2410.02298*.
- Xinyue Shen, Zeyuan Chen, Michael Backes, Yun Shen, and Yang Zhang. 2023. "do anything now": Characterizing and evaluating in-the-wild jailbreak prompts on large language models. *arXiv preprint arXiv:2308.03825*.
- Xiongtao Sun, Deyue Zhang, Dongdong Yang, Quanchen Zou, and Hui Li. 2024. Multi-turn context jailbreak attack on large language models from first principles. *arXiv preprint arXiv:2408.04686*.
- Rohan Taori, Ishaan Gulrajani, Tianyi Zhang, Yann Dubois, Xuechen Li, Carlos Guestrin, Percy Liang, and Tatsunori B. Hashimoto. 2023. Stanford alpaca: An instruction-following llama model. [https://github.com/tatsu-lab/stanford\\_alpaca](https://github.com/tatsu-lab/stanford_alpaca).

Hugo Touvron, Louis Martin, Kevin Stone, Peter Albert, Amjad Almahairi, Yasmine Babaei, Nikolay Bashlykov, Soumya Batra, Prajjwal Bhargava, Shruti Bhosale, et al. 2023. Llama 2: Open foundation and fine-tuned chat models. *arXiv preprint arXiv:2307.09288*.

Laurens Van der Maaten and Geoffrey Hinton. 2008. Visualizing data using t-sne. *Journal of machine learning research*, 9(11).

Yihan Wang, Zhouxing Shi, Andrew Bai, and Chojui Hsieh. 2024. [Defending llms against jailbreaking attacks via backtranslation](#). *Preprint*, arXiv:2402.16459.

Yueqi Xie, Minghong Fang, Renjie Pi, and Neil Gong. 2024. [GradSafe: Detecting jailbreak prompts for LLMs via safety-critical gradient analysis](#). In *Proceedings of the 62nd Annual Meeting of the Association for Computational Linguistics (Volume 1: Long Papers)*, pages 507–518, Bangkok, Thailand. Association for Computational Linguistics.

Yueqi Xie, Jingwei Yi, Jiawei Shao, Justin Curl, Lingjuan Lyu, Qifeng Chen, Xing Xie, and Fangzhao Wu. 2023. Defending chatgpt against jailbreak attack via self-reminders. *Nature Machine Intelligence*, 5(12):1486–1496.

Zhangchen Xu, Fengqing Jiang, Luyao Niu, Jinyuan Jia, Bill Yuchen Lin, and Radha Poovendran. 2024. [SafeDecoding: Defending against jailbreak attacks via safety-aware decoding](#). In *Proceedings of the 62nd Annual Meeting of the Association for Computational Linguistics (Volume 1: Long Papers)*, pages 5587–5605, Bangkok, Thailand. Association for Computational Linguistics.

Zhiyuan Yu, Xiaogeng Liu, Shunning Liang, Zach Cameron, Chaowei Xiao, and Ning Zhang. 2024. Don’t listen to me: Understanding and exploring jailbreak prompts of large language models. In *33rd USENIX Security Symposium (USENIX Security 24)*, Philadelphia, PA. USENIX Association.

Chongwen Zhao, Zhihao Dou, and Kaizhu Huang. 2024a. Eeg-defender: Defending against jailbreak through early exit generation of large language models. *arXiv preprint arXiv:2408.11308*.

Wei Zhao, Zhe Li, Yige Li, Ye Zhang, and Jun Sun. 2024b. Defending large language models against jailbreak attacks via layer-specific editing. *arXiv preprint arXiv:2405.18166*.

Zhenhong Zhou, Haiyang Yu, Xinghua Zhang, Rongwu Xu, Fei Huang, and Yongbin Li. 2024. How alignment and jailbreak work: Explain llm safety through intermediate hidden states. *arXiv preprint arXiv:2406.05644*.

Andy Zou, Zifan Wang, J. Zico Kolter, and Matt Fredrikson. 2023. [Universal and transferable adversarial attacks on aligned language models](#). *Preprint*, arXiv:2307.15043.

## A Statistics of Observed Data

We present the statistics of our data for observation experiments as Table 3.

Type	Samples
Benign samples	20,000
Harmful samples	8,556
<b>Jailbreak samples</b>	
AdvPrompter	1,872
AutoDAN	520
COLD-Suffix	436
ArtPrompt	361
GCG-Individual	340
GCG-Universal	312
PAIR	110
<b>Total</b>	<b>32,507</b>

Table 3: Statistics of observation experiments in §3. The attacked samples are derived from part or all of the samples from AdvBench(Zou et al., 2023).

## B Full View of Activation Space

We visualize activation spaces of all layers in Vicuna-7B-v1.3, as shown in Figure 7, Figure 8 and Figure 9.

## C Supplementary Experiments

### C.1 Data Augmentation Experiment

We show that by adopting the same method as Shen et al. (2024), we can draw a different conclusion by scaling up data. Shen et al. (2024) state jailbreak happens by posing jailbreak activations between benign and harmful activations in middle and deep layers. Following Shen et al. (2024), we randomly select 60 samples for each type of activation and conduct t-SNE on layer 14, as shown in the left part of 5. Jailbreak activations are between harmful and benign samples, which is in agreement with Shen et al. (2024). When scaling up each type of activation to 500 samples, jailbreak activations seem to cluster on the harmful activation side, as shown in the right part of 5. Therefore, jailbreak activations are not always between harmful and benign activations in deeper layers.

### C.2 Inclusion Ratio Experiments

For a layer  $l$ , to measure the portion of a set of jailbreak activations  $A^l = \{a_0^l, a_1^l, \dots, a_n^l\}$  that resides in harmful activation space, we propose an inclusion ratio. Based on 8,556 harmful samples gathered in Table 3, we calculate a ball that covers 80% activations. The center of the ball is  $\mu_{\mathcal{D}}^l$ , and the radius of the ball is denoted as  $r_{\mathcal{D}}^l$ .

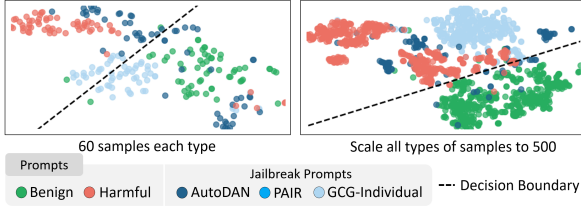


Figure 5: t-SNE visualization of activations in layer 14. Left: Results with 60 samples per type following (Shen et al., 2024), showing jailbreak activations between harmful and benign activations. Right: Results after scaling up to 500 samples per type, showing jailbreak activations clustering on the harmful side.

Then, we calculate the portion of  $A^l$  which are contained within the ball:

$$\rho_{\text{inclusion}}^l = \frac{|\{a_i^l \in A^l \mid \|a_i^l - \mu_{\mathcal{D}}^l\|_2 \leq r_{\mathcal{D}}^l\}|}{|A^l|},$$

where  $\|a_i^l - \mu_{\mathcal{D}}^l\|_2$  is the distance between the activation and the center. We calculate inclusion ratios of different types of jailbreak activations, with three representative types shown in Figure 1. We then apply ABD on all types of jailbreak activations and calculate their inclusion ratios. Notably, despite different types of jailbreaks, they all achieve an inclusion ratio of 100% with ABD applied, which verifies the effect of our method.

## D Supplementary Illustration on ABD

### D.1 Visualization of the penalty function.

A visualization of penalty functions are shown in Figure 6. The penalty function is symmetric about  $(\mu_{\mathcal{D}}^l, \mu_{\mathcal{D}}^l)$ . Figure 6(a) and Figure 6(b) presents the change in the range  $[\mu_{\mathcal{D}}^l - b^l, \mu_{\mathcal{D}}^l + b^l]$ , where  $x' \approx x$ . A larger  $\beta^l$  results in the larger little-perturbed region. Figure 6(a) and Figure 6(c) presents the change in the range of  $x'$ . When  $\alpha^l$  increases,  $x'$  is confined within a wider range of values.  $\alpha^l$  and  $\beta^l$  collaboratively determines behaviors of the penalty function.

### D.2 ABD Optimization Settings

**Validation data.** To make validation data, we adopt GCG-Universal (Zou et al., 2023). We optimize a common suffix for all 400 samples, with `n_steps=1`, `batch_size=512`.

To ensure efficiency, in each iteration of optimization, we select a batch of harmful prompts from the 400 entries as  $\mathcal{S}_{\text{val}}$ . We initially set the batch size to 15. In most cases

$\mathcal{L}_{\text{Robust}}(\Theta, M|\mathcal{S}_{\text{val}}) < 0.9$ , and the optimization process continues to the next iteration. If  $\mathcal{L}_{\text{Robust}}(\Theta, M|\mathcal{S}_{\text{val}}) \geq 0.9$ , due to the potential regional optimal, we iteratively increase the batch size by ten and reformulate  $\mathcal{S}_{\text{val}}$  to test again. This process ends if 1) the calculated  $\mathcal{L}_{\text{Robust}} < 0.9$  or 2) batch size reaches 50.

**Initial values.** To prevent the futile search of the optimizer, we set valid initial values before optimization: for  $i \in \{2, 12\}$ ,  $m_i = 1, \alpha_i = 1, \beta_i = 0.5, k_i = 0.5$ ; for  $i \notin \{2, 12\}$ ,  $m_i = \alpha_i = \beta_i = k_i = 0$ .

**Optimizing framework.** We adopt Optuna (Akiba et al., 2019) as our framework of optimization. We follow Optuna’s default settings, i.e., Gaussian process-based Bayesian Optimization.

## E Supplementary Illustration on Experiments

### E.1 Generation Configs

When conducting experiments, we directly utilize most of the original configurations of Vicuna-7B-v1.3 and Llama2-7B-chat. Specifically, we set `max_new_tokens=128`. We find that the proper functioning of these LLMs largely depends on the chat template of the inputs. We apply chat templates in `fastchat v0.2.36` by:

```
fastchat.model.get_conversation_template(
    template_name).
```

We set `template_name="vicuna"` for Vicuna-7B-v1.3 and `template_name="llama-2"` for Llama2-7B-chat.

### E.2 Jailbreak Methods

**GCG-Individual and GCG-Universal** (Zou et al., 2023) are optimization-based jailbreak attacks. They build towards an objective to repeat the prompt affirmatively and optimize a suffix based on a Greedy Coordinate Gradient-based search. The model would likely repeat the prompt affirmatively and generate harmful content with the suffix added behind the original prompt. GCG-Individual focuses on generating a tailored suffix designed specifically for a particular prompt. In contrast, GCG-Universal seeks to identify a generalized suffix that can be applied across multiple prompts, enabling it to deceive the model in a broader range of scenarios.



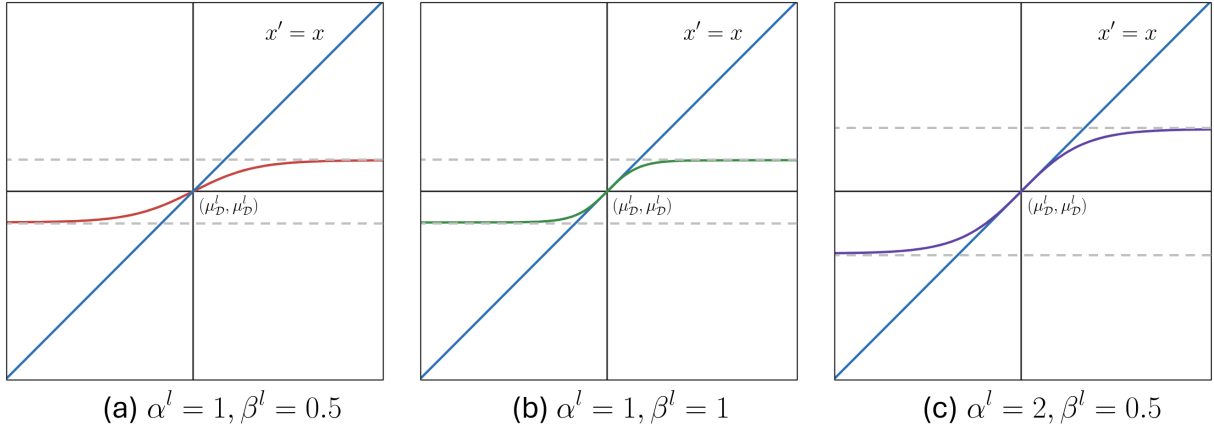


Figure 6: Penalty functions under different  $\alpha^l, \beta^l$  compared with  $x' = x$ .

**AutoDAN** (Liu et al., 2024b) utilize a meticulously designed hierarchical genetic algorithm and generate stealthy jailbreak prompts. The generated prompts are highly readable and transferable.

**PAIR** (Chao et al., 2023) is a jailbreak method that leverages an attacker LLM aiming at making the target LLM answer harmful prompts. The attacker LLM iteratively queries the target LLM to update and refine a candidate jailbreak prompt.

**DeepInception** (Li et al., 2023) proposes a simple method that uses the personification ability of LLMs. It creates a virtual and layered scene, allowing the model to find flexible ways to bypass usage controls in normal situations.

### E.3 Defense Methods

**PPL** (Alon and Kamfonas, 2023) discovers that jailbreak prompts often lead to high perplexity values in LLMs. It, therefore, involves adding a classifier trained on perplexity and text length at the end of LLMs. The classifier can serve as a filter to avoid outputting potentially harmful answers.

**Paraphrase** (Jain et al., 2023) defense LLMs by making them paraphrase their inputs, avoiding deception caused by potential adversarial jailbreak suffixes within original inputs.

**Retokenization** (Jain et al., 2023) disrupts adversarial suffixes by retokenizing the input sequence, breaking tokens apart, and re-representing them with smaller tokens.

**SafeDecoding** (Xu et al., 2024) is a safety-aware decoding strategy. It mitigates jailbreak attacks by amplifying the probabilities of safety disclaimer tokens among top-ranked tokens and attenuating

the probabilities of harmful token sequences, ensuring LLMs generate helpful and harmless responses.

**Self-Exam** (Phute et al., 2023) triggers the LLMs’ awareness of safety issues by adding a pre-defined prompt template, asking LLMs to examine if their outputs are safe.

**Self-Reminder** (Xie et al., 2023) defends the LLMs by adding a system prompt specifically emphasizing potential safety issues to prevent the model from outputting harmful responses.

### E.4 Metrics

#### E.4.1 Calculating DSR

We use Dic-Judge (Zou et al., 2023) to calculate DSR. Dic-Judge detects the presence of pre-defined refusal strings in the outputs of LLMs. Given a jailbreak query as input, if a particular refusal string is detected in the outputs, we consider the model successfully refuses to answer the question, thereby achieving the goal of defense; otherwise, the model is deemed to be deceived by the jailbreak inputs. DSR is defined as follows:

$$\text{DSR} = \frac{|\{\text{responses containing refusal strings}\}|}{|\{\text{input jailbreak queries}\}|}.$$

We adopt refusal strings as proposed by Xu et al. (2024), presented in Table

#### E.4.2 Calculating Overall Scores

We use Runtime per Query and overall averaged Just-Eval scores to calculate overall scores:

$$\text{Overall} = [1 - \text{Norm}(t) + \text{Norm}(\text{Avg.})]/2,$$

where  $t$  is Runtime per Query and Avg. represents overall averaged Just-Eval scores. 4.

---

**Refusal Strings**

---

I'm sorry  
Sorry  
I am sorry  
I apologize  
As an  
As an AI  
I'm an  
I'm just  
As a language model  
As an Assistant  
I cannot  
I do not  
It is not</s>  
It is not appropriate  
I'm unable to  
I am unable to  
I am not allowed to  
I am an AI language model

---

---

Table 4: Refusal strings.

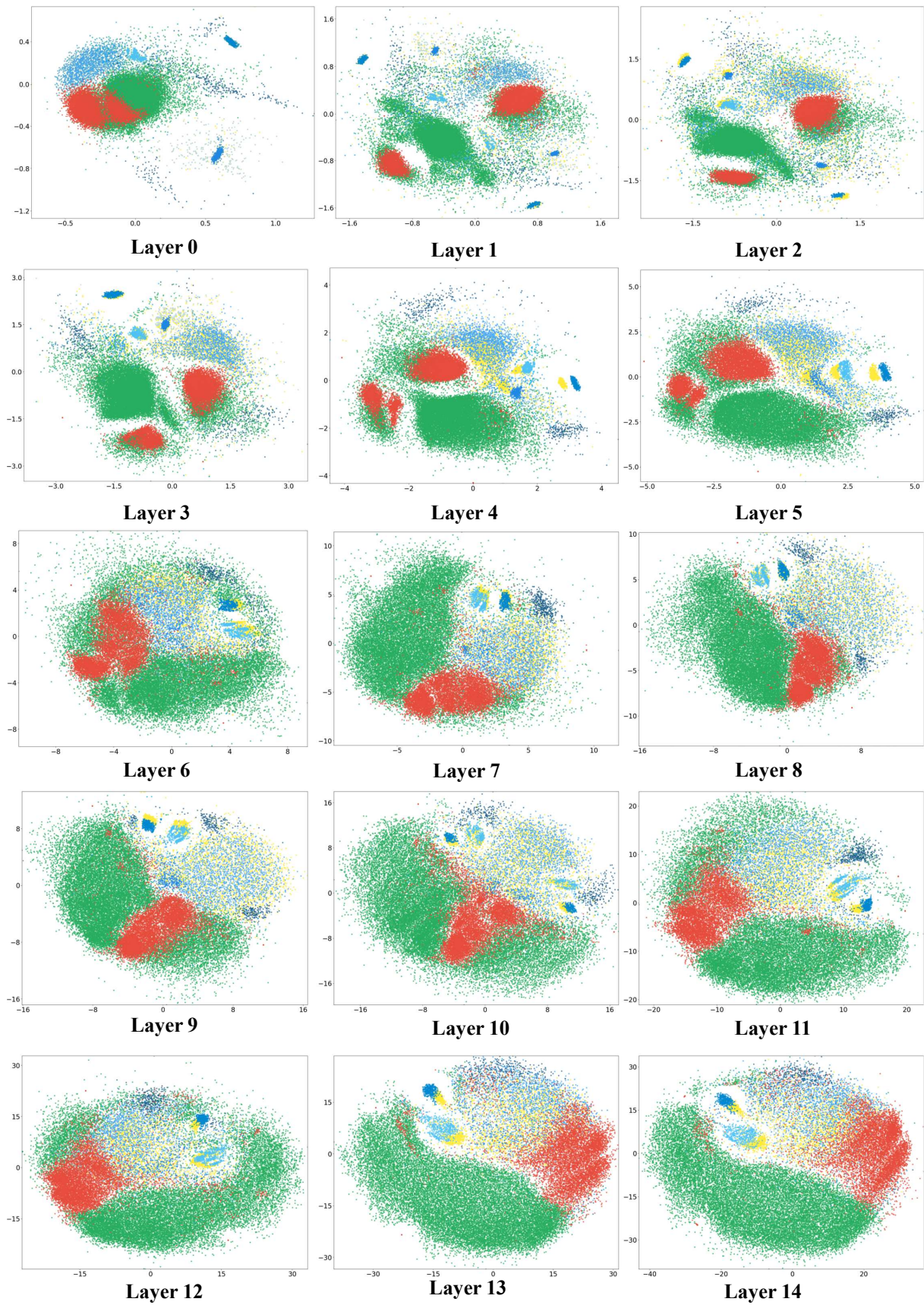


Figure 7: Activation spaces from layer 0 to layer 14.



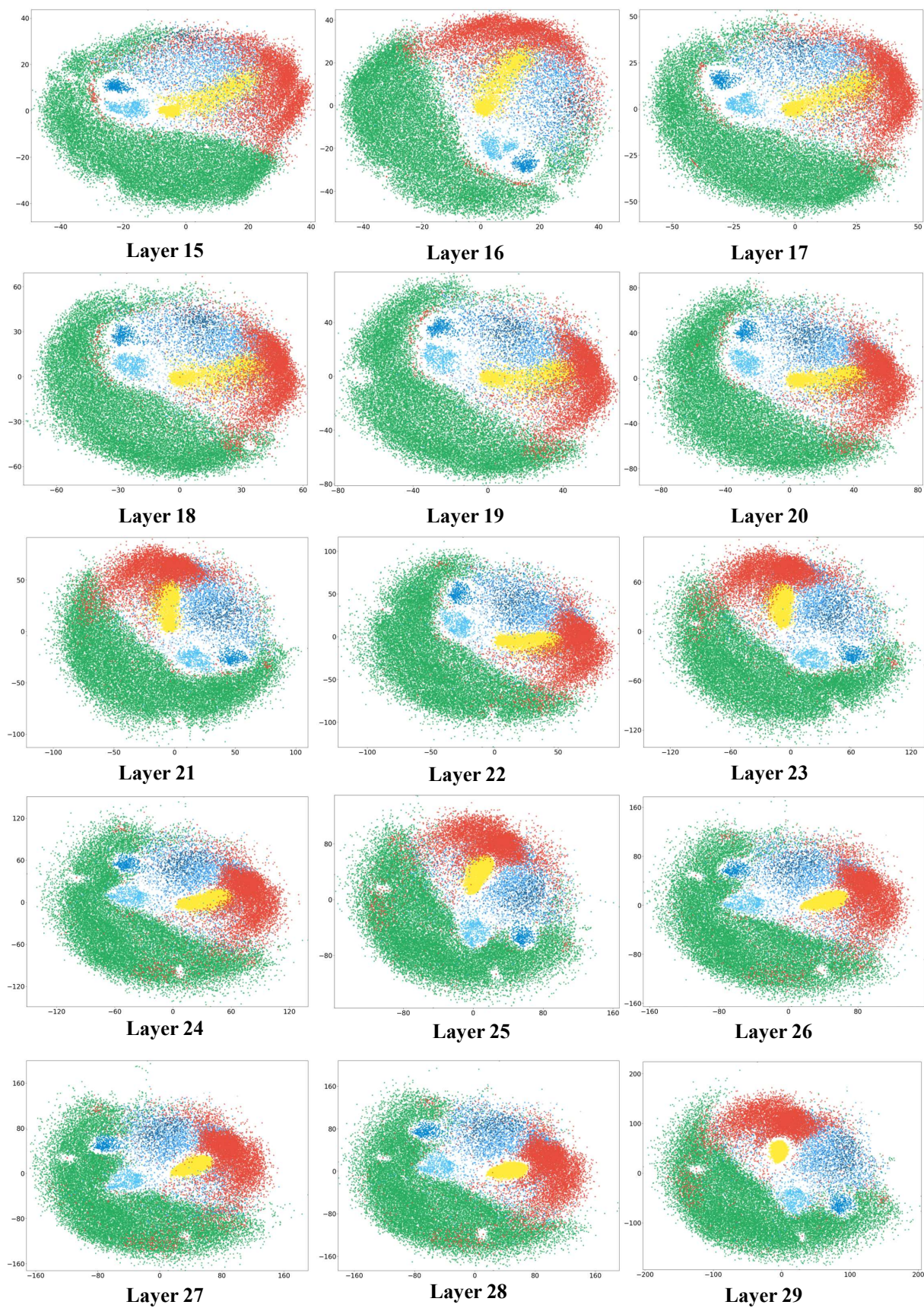


Figure 8: Activation spaces from layer 15 to layer 29.



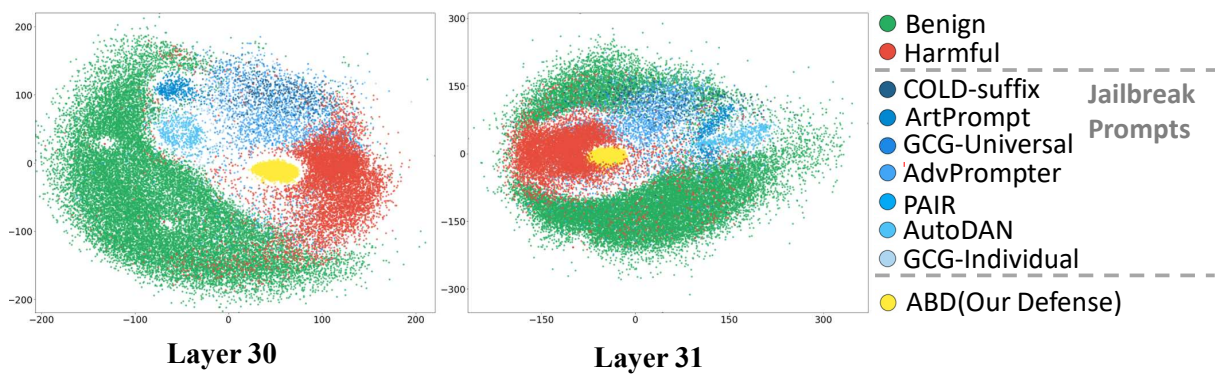


Figure 9: Activation spaces from layer 30 to layer 31.